



Article

Cite this article: Fees A, van Herwijnen A, Lombardo M, Schweizer J (2025) Towards a model of glide-snow avalanche occurrence using in-situ soil and snow measurements. *Journal of Glaciology* **71**, e119, 1–12. <https://doi.org/10.1017/jog.2025.10097>

Received: 4 June 2025

Revised: 25 September 2025

Accepted: 26 September 2025

Keywords:

avalanche; avalanche forecasting; glide-snow avalanche; interfacial water; snow; snow gliding; snowpack; snow-soil interface

Corresponding author: Alec van Herwijnen;
Email: vanherwijnen@slf.ch

Towards a model of glide-snow avalanche occurrence using in-situ soil and snow measurements

Amelie Fees, Alec van Herwijnen , Michael Lombardo and Jürg Schweizer 

WSL Institute for Snow and Avalanche Research SLF, Davos, Switzerland

Abstract

Glide-snow avalanches release at the soil-snow interface and are currently difficult to predict. This is mostly due to a limited understanding of the release process and a lack of data, particularly of the snowpack and underlying soil conditions prior to release. Here, we synthesize the current process understanding on the source of interfacial water—a key factor in glide-snow avalanche release—in a simple explanatory model. The model classifies days with and without glide-snow avalanche activity using thresholds applied to proxies including snow liquid water content (LWC), soil temperature, soil LWC and meteorological parameters. These proxies were measured on Dorfberg (Davos, Switzerland) in the 2021/22 to 2023/24 seasons. The best-performing thresholds for the snow, soil and meteorological time series were determined through quasi-random sampling and were in line with previous field studies. Soil temperature and snow LWC were the most relevant variables to explain avalanche occurrence. These results demonstrate the importance of combining snow, soil and meteorological data for improving the forecasting of glide-snow avalanche activity.

1. Introduction

Our ability to predict glide-snow avalanches is currently limited (Jones, 2004). Avalanche warning services frequently issue the general warning “glide-snow avalanches are possible” over extended periods during the winter season. For instance, during the winter season 2023/24, the avalanche warning service in Switzerland forecasted glide-snow avalanches in the region of Davos for 82% of the days. Glide-snow avalanches were observed on 57% of these days (Zweifel and others, 2025). This overforecasting poses a challenge for avalanche control services in charge of road or ski resort safety due to a lack of reliable mitigation measures (Clarke and McClung, 1999; Sharaf and others, 2008; Simenhois and Birkeland, 2010), which necessitates costly closures (Humstad and others, 2018) or permanent protection measures. Thus, reliable forecasting is critical, but currently not possible due to a lack of fundamental understanding of the underlying processes leading to glide-snow avalanche release. Additionally, this lack of process understanding prohibits the assessment of how glide-snow avalanche activity may respond to climate change, despite a common perception among practitioners that glide activity is increasing under warming conditions. To the best of our knowledge, no systematic studies have yet addressed this issue, in large part due to the absence of models capable of predicting glide-snow avalanche release.

It is generally accepted that the loss of support at the soil–snow interface, which leads to glide-snow avalanche release, is connected to the presence of interfacial water (Clarke and McClung, 1999). Based on the source of interfacial water, glide-snow avalanches can be classified into interface and surface events (Fees and others, 2025c). In interface events, the interfacial water originates from the soil-snow interface due to processes such as geothermal melting (McClung, 1987; Newsely and others, 2000; Höller, 2001) or capillary suction of water from the soil into the snowpack (Mitterer and Schweizer, 2012; Lombardo and others, 2025). As interface events are associated with a dry snowpack with temperatures below zero degrees, they are also commonly referred to as “cold” events (Clarke and McClung, 1999). The driving processes can be observed through proxies such as (i) a high soil temperature (Ceaglio and others, 2017; Fromm and others, 2018) which favors melting of the lowermost snowpack or (ii) high soil liquid water content (LWC) which is required for capillary suction (Lombardo and others, 2025). Studies have also found that snow loading is related to the release of interface events (in der Gand and Zupančič, 1966; Höller, 2014; Dreier and others, 2016; Fees and others, 2025a).

For surface events, the water originates from the snow surface and percolates through the (locally) isothermal snowpack to the snow-soil interface. As the snowpack is usually isothermal, these events are also commonly referred to as “warm” events (Clarke and McClung, 1999). These events are typically associated with (i) positive air temperatures (Dreier and others, 2016; Ceaglio and others, 2017) and high incoming long-wave radiation (Dreier and others, 2016),

© The Author(s), 2025. Published by Cambridge University Press on behalf of International Glaciological Society. This is an Open Access article, distributed under the terms of the Creative Commons Attribution licence (<http://creativecommons.org/licenses/by/4.0>), which permits unrestricted re-use, distribution and reproduction, provided the original article is properly cited.

[cambridge.org/jog](https://www.cambridge.org/jog)



which facilitate snow melt, (ii) high soil LWC (Fees and others, 2025a), which indicates the percolation of meltwater from the snow into the soil, or (iii) rainfall onto the snow cover hours to days before avalanche release (Stimberis and Rubin, 2011). Field observations have also indicated that a higher snow liquid water content is associated with surface events rather than interface events (Maggioni and others, 2019; Fees and others, 2025a).

Several field studies have highlighted the correlation of snow LWC, soil LWC and soil temperature with glide-snow avalanche release (Höller, 2001; Maggioni and others, 2019; Fees and others, 2025a). However, these studies of combined temperature and LWC data for both the soil and snow are scarce. This is likely because measuring snow LWC requires manual snow profiles and is time-consuming. As a result, previous studies focused on meteorological parameters to predict days with glide-snow avalanches using multivariate statistical methods (e.g., logistic or multiple linear regression, random forest) (Dreier and others, 2016; Resch and others, 2023). Dreier and others (2016) showed promising results towards forecasting “warm” events using the correlation of air temperature and incoming long-wave radiation with rain and snowpack meltwater formation. However, forecasting “cold” (interface) events remained a challenge, due to a lack of relevant information (modeled or measured) from the processes at the snow-soil interface (Dreier and others, 2016).

This study aims to explore the potential of combining extensive soil, snow and meteorological data with our current process understanding of glide-snow avalanches into a simple explanatory model of glide-snow avalanche occurrence. The model classifies days with and without glide-snow avalanches using thresholds applied to proxies of interfacial water formation, such as snow and soil LWC. These proxies have been observed in recent field studies (Ceaglio and others, 2017; Fromm and others, 2018; Maggioni and others, 2019; Fees and others, 2025a). We optimized the thresholds using the extensive dataset of snow and soil measurements on Dorfberg for the seasons 2021/22 to 2023/24. Our goal was to demonstrate the promising potential of combining a process-based model with data measured at the soil-snow interface towards the prediction of glide-snow avalanche occurrences.

2. Methods

2.1. Input data: Dorfberg field site

The model was based on daily values of eight time series describing snow, soil and weather conditions. The input data originated from Dorfberg, the mostly southeast-facing hillslope of the Salezer Horn (1650 to 2100 m a.s.l., Davos, Switzerland, Fig. 1). This field site combines well-recorded historical glide-snow avalanche activity through time-lapse photography (seasons 2008/09 to 2023/24, Fees and others (2025c)) and recent soil and snow monitoring in an avalanche-prone slope (seasons 2021/22 to 2023/24; Fees and others (2025a)). Hence, for seasons 2021/22 to 2023/24, we collected a comprehensive dataset of glide-snow avalanche activity as well as soil, snow and meteorological measurements. A winter season was defined as 1 November through 1 May. For season 2021/22, the start of the season was defined as 23 November 2021 because this was the first day with soil measurements.

2.1.1. Glide-snow avalanche activity

Glide-snow avalanche activity on Dorfberg was extracted from time-lapse photographs recorded at a time interval of 5 minutes (Fees and others, 2025c). Avalanche activity was classified

as days with at least one glide-snow avalanche release (avalanche day, $n = 45$) and days without a glide-snow avalanche release (non-avalanche day, $n = 479$). The glide-snow avalanche activity in the three winter seasons 2021/22 to 2023/24 varied substantially. Season 2021/22 was characterized by an average number of glide-snow avalanche days ($n = 7$), which occurred in two distinct clusters in early winter and spring. Season 2022/23 was characterized by a lack of glide-snow avalanche activity, with only one observed glide-snow avalanche and one glide-snow avalanche day ($n = 1$). Season 2023/24 was characterized by an above-average number of glide-snow avalanche days ($n = 37$). The three winter seasons were described in detail by Fees and others (2025a).

2.1.2. Soil measurements

Soil liquid water content (LWC_{soil}) and temperature (T_{soil}) were monitored in a slope with many documented glide-snow avalanches on Dorfberg called the Seewer Berg (1765–1818 m a.s.l., Fig. 1). This was done using a grid of 20 sensors across the slope (TEROS11, Meter Group (2025)). Every sensor was installed at a soil depth of 5 cm such that the full sensor measurement volume of 1010 cm³ (Meter Group, 2025) was covered by soil. Measurements were recorded every 15 minutes. For this study, we calculated the mean of T_{soil} and LWC_{soil} across all sensors. This removed location-specific temporal variations that can be introduced by local soil inhomogeneities. For details on the sensor installation and setup, see Fees and others (2025a). The model uses the daily mean values for soil temperature (T_{soil}) and soil LWC (LWC_{soil}) as inputs (Table 1).

2.1.3. Snow measurements

Manual (bi)weekly snow profiles (Fierz and others, 2009) were recorded to determine the interfacial snow liquid water content in a reference location. The reference location refers to a small slope 100 m northwest of the Seewer Berg slope (Fig. 1). From the manual snow profile, we derived the interfacial snow liquid water content (LWC_{snow}) of the lowermost 20 cm of the snowpack. The LWC_{snow} was measured at height increments of 5 to 10 cm by recording snow density, relative permittivity and snow temperature. The relative permittivity was recorded with a capacitive sensor (Denoth, 1994) and snow density was determined as the mean of two density measurements per height using a density cutter (100 cm³). LWC_{snow} was then calculated as the mean across all snow LWC measurements where the snow temperature was above -0.1°C . The model uses daily LWC_{snow} values which were interpolated with nearest neighbor interpolation (Table 1).

2.1.4. Meteorological measurements and SNOWPACK simulation

Meteorological parameters were recorded at three automated weather stations (AWS) ranging in elevation from Davos to Weissfluhjoch (1563–2536 m a.s.l.). The two IMIS stations Weissfluhjoch (id: WFJ2, 2536 m a.s.l.) and Madrisa (id: KLO2, 2147 m a.s.l.) were used to interpolate the meteorological parameters to the reference location (1840 m a.s.l.). The interpolation of the meteorological parameters was validated against the AWS Dorfberg (2140 m a.s.l., Fig. 1). The interpolated meteorological parameters were used for the SNOWPACK (Bartelt and Lehning, 2002) simulations using the bucket approach for water transport. The SNOWPACK simulations were validated against the manual snow profiles that were recorded at the reference site throughout season 2021/22. For details on the setup, limitations and validation of the SNOWPACK simulation, see Fees and others (2025c). Of

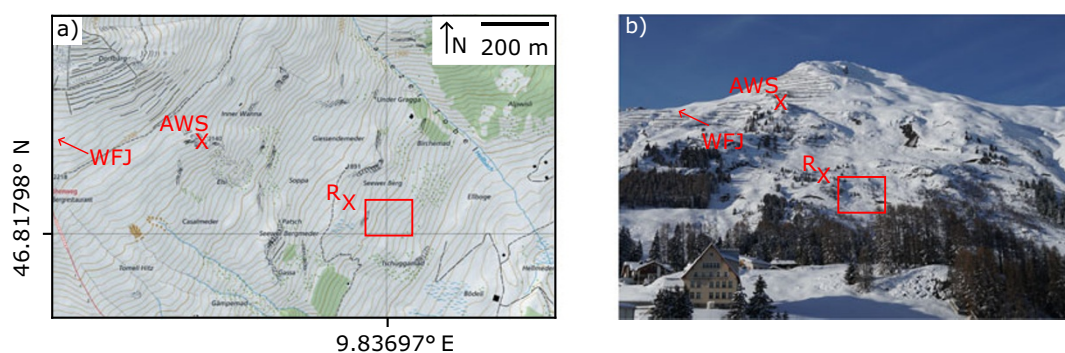


Figure 1. (a) Map and (b) picture of Dorfberg indicating the location of the weather station (AWS), the reference location (R), the Seewer Berg slope with the spatio-temporal monitoring setup (square) and the direction towards the Weissfluhjoch measurement site (WFJ). Map: Federal Office of Topography, WGS84.

Table 1. Overview of the input parameters, their source, data aggregation/interpolation and the corresponding model thresholds

Parameter	Unit	Source	Location	Time interval raw data	Data interpolation (I)/ aggregation (A)	Thresholds
Bulk snow density (ρ)	kg m ⁻³	SNOWPACK	Reference	10 min	(A): daily mean	t_ρ
Snow LWC (LWC_{snow})	%	Manual profile	Reference	5 to 9 days	(I): next neighbor	$t_{LWC \text{ interface}}, t_{LWC \text{ surface}}$
Snow height (HS)	cm	SNOWPACK	Reference	10 min	(A): daily mean	t_{HS}
3 day sum of new snow height (HN3d)	cm	SNOWPACK	Reference	10 min	(A): daily mean	t_{HN3d}
Temperature soil (T_{soil})	°C	20 sensors	Seewer Berg	15 min	(A): daily mean across sensors	$t_{T_{\text{soil}}}$
Soil LWC (LWC_{soil})	m ³ m ⁻³	20 sensors	Seewer Berg	15 min	(A): daily mean across sensors	$t_{LWC_{\text{soil}}}$
Rain (P)	mm	SNOWPACK	Reference	10 min	(A): daily mean	t_P, t_{duration}
Air temperature (T_{air})	°C	SNOWPACK	Reference	10 min	(A): daily mean	$t_{T_{\text{air}}}$

note, SNOWPACK was only used to distinguish between interface and surface events; accordingly, we did not include a soil layer in the simulations, and simulated LWC values at the snow–soil interface are therefore not representative of real conditions. The simulation was run at a time interval of 10 minutes, and values were aggregated to daily mean values. The classification model for glide-snow avalanche occurrence uses five daily time series as inputs which consist of: air temperature (T_{air}), snow height (HS), 3 day sum of new snow height (HN3d), bulk snow density (ρ), and rain amounts (P) (Table 1).

2.2. Model setup

Given the relatively small sample size of observed glide-snow avalanches in our dataset, we adopted a threshold-based classification model grounded in current process understanding, since more data-intensive machine learning approaches (e.g. logistic regression, random forests, neural networks) were not appropriate. The classification model provides a binary classification into days with and without glide-snow avalanches. The classification is based on daily values of eight time series, which were selected based on the current process understanding of the formation of water at the soil-snow interface (Fees and others, 2025a). These time series include bulk snow density (ρ), snow height (HS), 3 day sum of new snow height (HN3d), air temperature (T_{air}) and the amount of rain (P) as simulated using SNOWPACK, snow LWC (LWC_{snow}) measured in the manual snow profile and soil LWC (LWC_{soil}), soil temperature (T_{soil}) from the sensor grid (Table 1, Subsection 2.1). Ten thresholds (t , Table 1) were applied to evaluate interfacial water availability and additional critical conditions (Fig. 2). The evaluation was separated into the three major processes that we assumed contributed water to the soil-snow interface: geothermal heat, snow surface melt and rain. For every process, there are up

to three boolean evaluations based on the thresholds (t), which are defined below. The model returns an avalanche day (boolean) if at least one process classified the day as a glide-snow avalanche day. In addition, the avalanche day is labeled based on the underlying process into interface, surface, or mixed event. The interface event label is applied if geothermal heat was the only contributing process. The surface event label is applied if melt and/or rain were the contributing processes. The mixed event label is applied if geothermal heat and either melt and/or rain were contributing processes.

In detail, the evaluation by process was implemented as follows:

(i) Geothermal heat: The availability of sufficient interfacial water was determined based on the snowpack bulk density ($\rho < t_\rho$) and interfacial snow LWC ($LWC_{\text{snow}} > t_{LWC \text{ interface}}$). Potentially critical conditions were implemented as a threshold on high soil temperature ($T_{\text{soil}} > t_{T_{\text{soil}}}$) and one threshold on snow loading ($HN3d > t_{HN3d}$). If more than one threshold was reached, the day was classified as an avalanche day.

(ii) Snow surface melt: The availability of interfacial water was determined by a high bulk density ($\rho > t_\rho$) and a sufficient amount of interfacial snow LWC ($LWC_{\text{snow}} > t_{LWC \text{ surface}}$). Potentially critical conditions were implemented as a threshold on high soil LWC ($LWC_{\text{soil}} > t_{LWC_{\text{soil}}}$) and a threshold on high air temperatures ($T_{\text{air}} > t_{T_{\text{air}}}$). If more than one threshold was reached, the day was classified as an avalanche day.

(ii) Rain: Rain as a source of interfacial water was accounted for with two thresholds, which account for the amount of rain necessary for release and the delayed release of glide-snow avalanches up to several days after the rainfall. The first threshold sets the amount of rain necessary for rain events to occur ($P > t_P$). If this threshold was fulfilled, the second threshold (t_{duration}) was used to indicate for how many consecutive days after the rainfall days were classified as an avalanche day.

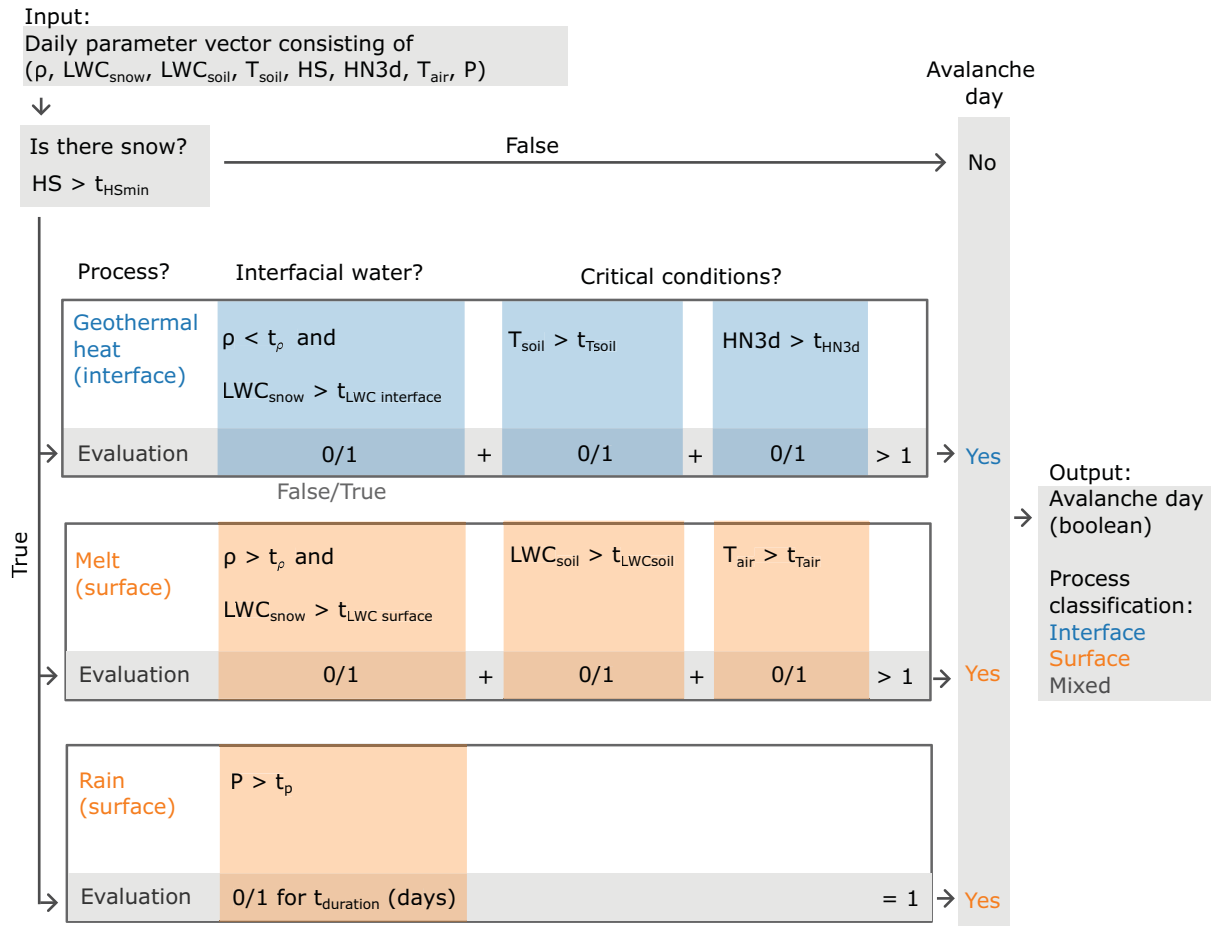


Figure 2. An overview of the model that classifies the daily parameter vector through thresholds (t) into avalanche days and non-avalanche days. The thresholds are based on the processes of geothermal melting, snow surface melt water formation and rain, which can contribute water at the soil-snow interface. In addition, an avalanche day is labeled based on the process(es) that resulted in the avalanche day classification. For an interface event (blue) this is due to geothermal heat, for a surface event (orange), this is due to melt or rain, and for a mixed event, it is due to geothermal heat and either melt or rain. Abbreviations are given in Table 1.

2.3. Threshold optimization

The binary classification of glide-snow avalanche occurrence depends on the choice of the threshold values and their combination (Table 1). We refer to the combination of all required thresholds as a threshold vector. Threshold vectors were generated through quasi-random sampling. The best threshold vector was determined based on the probability of detection (POD) and the false alarm rate (F), which are used in a ROC diagram (Wilks, 2011). These metrics are defined based on the number of avalanche days that were correctly classified by the model (true positive, TP), the number of non-avalanche days that were correctly classified (true negative, TN), the number of avalanche days that were incorrectly classified (false positive, FP) and the number of non-avalanche days that were incorrectly classified (false negative, FN). The probability of detection (or hit rate) was calculated as

$$POD = \frac{TP}{TP + FN}, \quad (1)$$

and the false alarm rate was calculated as

$$F = \frac{FP}{FP + TN}, \quad (2)$$

(Wilks, 2011).

A perfect model would result in a $POD = 1$ and $F = 0$.

To find the best-performing threshold vector, 2^{20} threshold vectors were generated quasi-randomly using Sobol's sequence (Sobol (1967), scipy implementation). Sobol's sequence, originally developed for variance decomposition in sensitivity analysis, ensures a more uniform coverage of the parameter space than purely random sampling, and thus improves the efficiency of the search for optimal threshold vectors. This results in threshold vectors consisting of 10 threshold values (Table 1) which are equally distributed over a 10-dimensional hypercube. The threshold values were sampled from the provided ranges in Table 2. Every threshold vector was evaluated based on the (minimum) Euclidean distance to the perfect model using the data of all seasons (2021/22 to 2023/24).

To investigate the relative influence of the various input parameters (snow, soil and meteorological data), we determined the best threshold vector while omitting one of the input parameters and repeated this leave-one-out procedure for each input parameter. The best threshold was repeatedly determined from the same 2^{15} quasi-randomly sampled threshold vectors. These threshold vectors also included the overall best threshold vector using all input parameters.

Table 2. Overview of threshold optimization. All parameters are daily mean values

Threshold	Unit	Range	Best threshold	Literature values
t_{ρ}	kg m ⁻³	[200, 350]	297	
$t_{LWC\ interface}$	%	[0, 6]	3	~3–5 (Fees and others, 2025a)
$t_{LWC\ surface}$	%	[6, 11]	6	~7 (Fees and others, 2025a)
t_{HS}	cm	20	20	
t_{HN3d}	cm	[10, 60]	29	80 (5-day sum; Dreier and others (2016))
t_{tsoil}	°C	[0, 5]	1.6	12 (not significant; Ceaglio and others (2017)) 2–3 (Fees and others, 2025a)
$t_{LWCsoil}$	m ³ m ⁻³	[0.350, 0.370]	0.369	0.5 (not significant; Ceaglio and others (2017)) 0.368 (mean of all surface events in Fees and others (2025a))
t_p	mm	[0, 1]	0.3	
$t_{duration}$	d	[0,4]	2	hours to days (Stimberis and Rubin, 2011; Fees and others, 2025a)
t_{Tair}	°C	[-1, 5]	1.9	1.6 (Dreier and others, 2016) 1.5 (Ceaglio and others, 2017)

3. Results

3.1. Model performance and best threshold

The model performance (POD, F) was highly dependent on the threshold vector (Fig. 3). The best threshold vector resulted in a POD of 0.91 and F of 0.21 (orange diamond in Fig. 3; Fig. 4d) and consisted of threshold values comparable to the literature and in line with the underlying processes (Table 2). The model performance separated by season showed that the best threshold vector performed well for season 2021/22 (POD = 1, F = 0.23, Fig. 4a) and season 2023/24 (POD = 0.92, F = 0.32, Fig. 4c). In season 2022/23, the threshold vector was not able to correctly predict the single avalanche that released on Dorfberg (Fig. 4b).

3.2. Process-based interpretability

The model was designed to provide a classification into days with and without glide-snow avalanches and apply a label based on the process (geothermal heat, melt and rain) that likely contributed the interfacial water. This model design allowed for interpretation

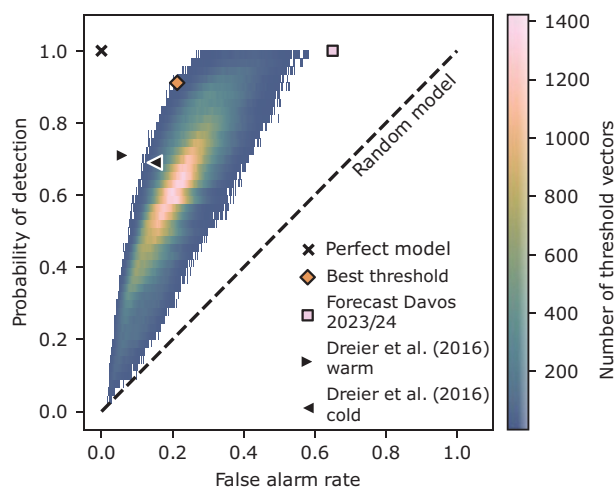


Figure 3. Threshold optimization for the best performance shown as ROC diagram. The model performance of all sampled threshold combinations is indicated as a heatmap, and the best threshold combination as an orange diamond. For context, we also provide the model performance of a perfect model (x), a random model (dashed 1:1-line), the model results reported by Dreier and others (2016) for “cold” (▲) and “warm” (◄) events, and the performance of the operational glide-snow avalanche forecast for the region of Davos as issued in the avalanche bulletin (pink square, season 2023/24).

of the model classification by using the labels (interface, surface, mixed) assigned to every avalanche day as well as access to all threshold evaluations (Fig. 5).

For example, season 2023/24 was characterized by persistent glide-snow avalanche activity on Dorfberg (Fig. 5a). The first window of glide-snow avalanche activity (25 Nov to 16 Dec 2023) was correctly identified by the model and labeled as interface events (Fig. 5a). This was due to sufficient snow LWC (Fig. 5b1,b2) combined with high soil temperature (Fig. 5b3) and repeated snow loading (Fig. 5b4).

The shift from interface events to surface events was predicted by the model on 17 December 2023 based on the increased bulk snow density ($\rho > 297 \text{ kg m}^{-3}$). Avalanche days were classified due to a sufficiently high measured snow LWC ($LWC_{\text{snow}} > 6\%$) in combination with high air temperatures ($T_{\text{air}} > 1.9^\circ\text{C}$) (Fig. 5c1,c2,c3).

The continuous glide-snow avalanche activity during season 2023/24 was interrupted from 27 December 2023 to 24 January 2024 when only one glide-snow avalanche released on Dorfberg (Fig. 5a). The model did not classify any glide-snow avalanche days during this time period because either the snow LWC was not sufficiently high for a surface event (Fig. 5b2) or no additional critical conditions for surface melt, such as high air temperature or soil LWC (Fig. 5c3, c4), were fulfilled.

A rain event occurred on 24 January 2024 (Fig. 5d,d1) which was captured by the model due to the amount of precipitation (Fig. 5d, d1). Due to the time threshold ($t_{\text{duration}} = 2$ days) both days, 24 and 25 January, were classified as surface events. High glide-snow avalanche activity was observed on Dorfberg on 25 January (Fig. 5a).

Intermittent glide-snow avalanche days occurred from 3 to 18 February 2024 (Fig. 5a). This was well captured by the model due to high air temperatures (Fig. 5c3) coinciding with sufficient snow LWC (Fig. 5c2). Beginning on 3 February 2024, most glide-snow avalanche days were labeled as surface events. However, a few days were labeled as interface events (e.g. 25 Feb, 19 and 20 Mar 2024) due to the increasing soil temperatures measured in the Seewer Berg slope, as it was intermittently covered by snow due to recent avalanche releases on the slope in combination with snow melt. As a result, the interface labels during this time period may not correctly reflect the processes leading to glide-snow avalanche release at higher elevations.

Overall, the model was able to correctly classify a large number of glide-snow avalanche days throughout season 2023/24. But more importantly, for a season with persistent glide-snow avalanche activity, the model was also able to capture the (short)

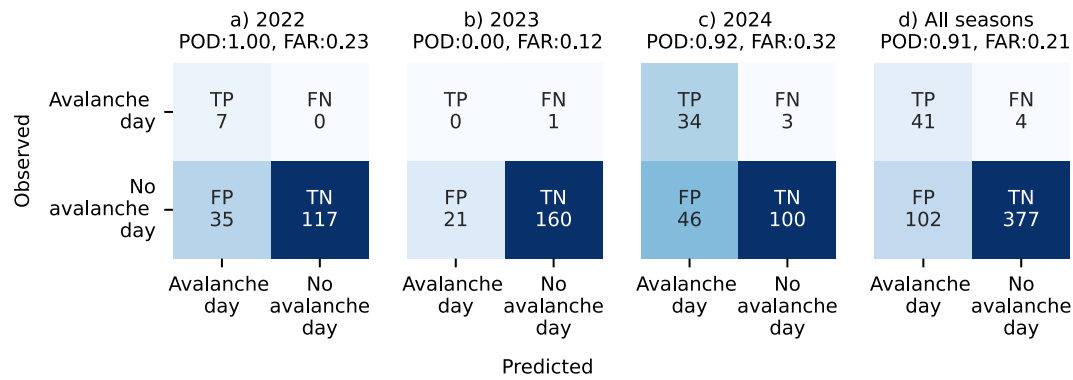


Figure 4. Confusion matrices based on the best threshold vector for every season (a–c) and all seasons combined (d).

time periods without glide-snow avalanche activity reasonably well. For season 2021/22 and season 2022/23 the model classification is given in the Appendix (Fig. A1, A2).

3.3. Relative dependence of model performance on input parameters

The relative effects of the input parameters on model performance were assessed by removing one parameter at a time and then optimizing the threshold vector again. The omission of LWC_{soil} and P had little effect on model performance (Fig. 6). The omission of T_{air} , T_{soil} , ρ , or LWC_{snow} resulted in a more prominent decrease in model performance (Fig. 6). The best threshold vectors after the omission of one input time series at a time are provided in the Appendix (Table A1).

4. Discussion

The aim of this study was to show that extensive soil, snow and meteorological monitoring, in combination with process understanding, can improve the classification of glide-snow avalanche occurrence in avalanche days and non-avalanche days. We synthesized the current process understanding on the formation of interfacial water and relevant proxies for interface and surface events in a binary classification model. The model thresholds were optimized for best performance based on data from three winter seasons. These seasons cover below-average (2022/23), average (2021/22), and above-average (2023/24) glide-snow avalanche activity on Dorfberg. While the model performed well for seasons with average and above-average glide-snow avalanche activity (Fig. 4a,c), it was not able to reproduce the single avalanche day in season 2022/23 (Fig. 4b). This misclassification is not surprising since this avalanche released at a location that is known for persistent soil wetness due to an underground water source. The model does not take groundwater and hydraulic processes, such as capillary suction, into account as a source of interfacial water.

4.1. Model validation

Given the limited data, we could not thoroughly validate the model, and the stated performance values are indicative at best. Nevertheless, as the avalanche activity during these three seasons varied, our results qualitatively show that the model performs reasonably well under many different conditions. More data from additional winters are needed to evaluate model robustness. With

a non-crossvalidated $POD = 0.91$ and $F = 0.21$, the performance is comparable to that of the statistical model presented by Dreier and others (2016), who classified glide-snow avalanche activity based on meteorological parameters at Dorfberg. The comparison with the operational glide-snow avalanche forecast for the region of Davos (season 2023/24) further suggests the potential of reducing the false alarm rate using combined soil, snow and meteorological measurements. However, confirming this will require a thorough investigation into scale effects and the representativeness of point measurements for larger forecast regions.

A strength of the model lies in the interpretability of the output. While data-based cross-validation is currently limited by scarce data, process-based validation using the labels assigned to glide-snow avalanche days was in line with our process understanding of the formation of interfacial water. The best-performing threshold vector was determined based on quasi-random sampling, and its components were in line with previous field observations on glide-snow avalanches. For example, the snow LWC threshold for interface events (3%) was lower than for surface events (6%), in line with recent studies (Maggioni and others, 2019; Fees and others, 2025a). For soil temperature, the best threshold was 1.6°C , comparable to literature values ranging from 0.5°C to 3°C (Ceaglio and others, 2017; Fees and others, 2025a). In addition, the threshold for air temperature, used as a proxy for surface melt, was 1.9°C even though the sampling interval also allowed for negative air temperatures. Positive air temperatures correspond with our expectation as a proxy for surface melt. The comparability of the sampled best threshold to field observations on glide-snow avalanches indicates that the chosen input variables for the model are promising proxies for the formation of interfacial water.

4.2. Input parameters

The time series used as inputs for the model originated from a unique and extensive dataset covering snow, soil and meteorological parameters on Dorfberg (Fees and others, 2025a).

Measurements of soil temperature and snow LWC contributed substantially to the overall model performance (Fig. 6). The relative importance of snow LWC may be due to the model setup, where it is needed as an input for both interface and surface events. Soil temperature only influenced the classification of days with interface events which on average account for a minority of glide-snow avalanche days (30%; (Fees and others, 2025c)). This indicates that T_{soil} has a substantial influence on the classification of interface events and is an important parameter to measure.

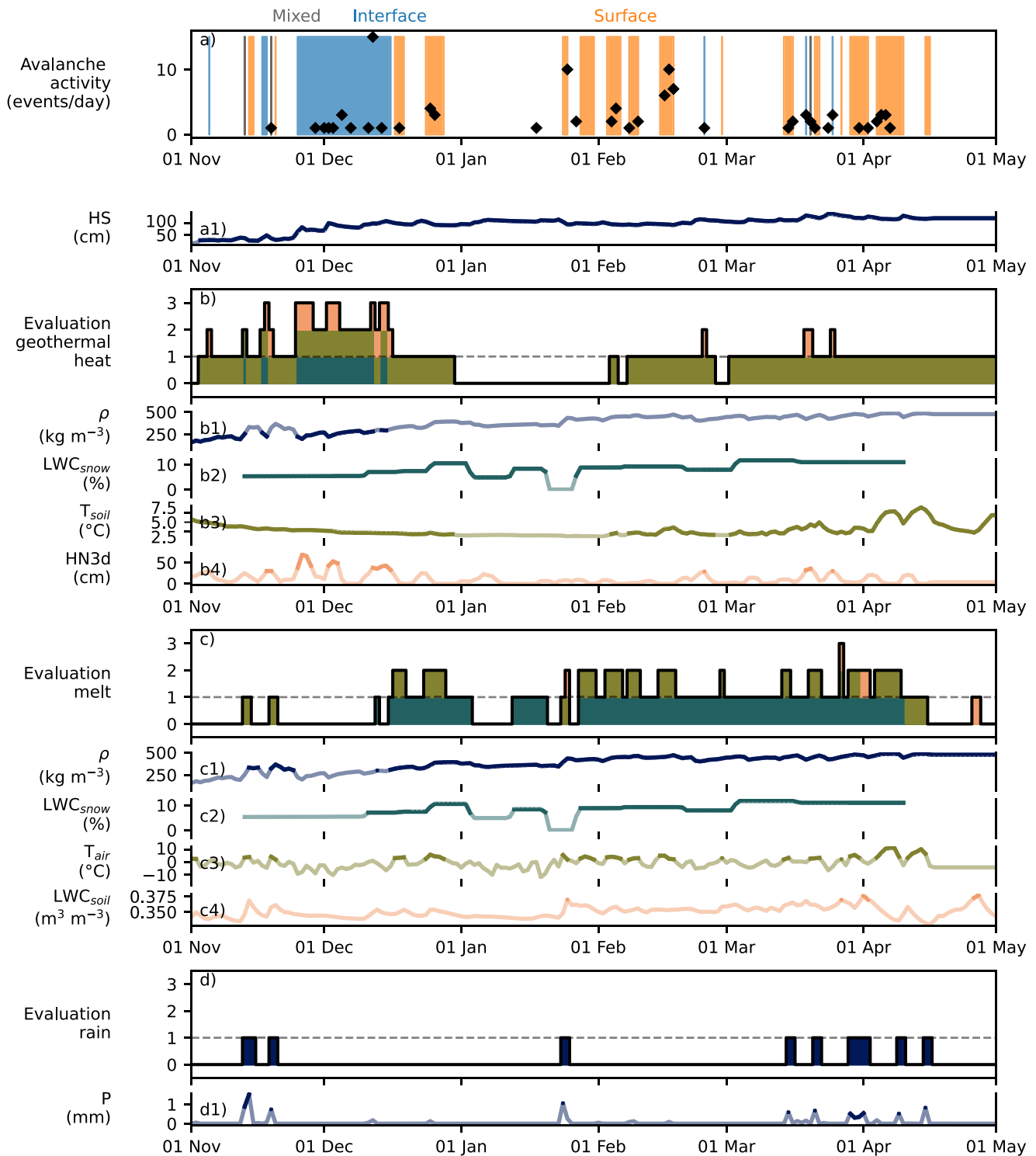


Figure 5. Model evaluation throughout season 2023/24. (a) Modeled glide-snow avalanche days (background color) in comparison to observed glide-snow avalanche activity on Dorfberg (black diamonds). This classification is based on three evaluations (b, c, d) which are based on thresholds on ten measured or simulated time-series (a1, b1-4, c1-4, d1). (a1) Snow height (HS) is a necessary requirement for glide-snow avalanches. In the time-series, a darker shade indicates that the condition (here: $HS > t_{HS}$) was met, while a lighter shade indicates that the condition was not met. (b) Evaluates the possibility of glide-snow avalanches based on geothermal heat. The background color visualizes the contributing thresholds consisting of (b1) bulk snow density in combination with (b2) snow LWC, (b3) soil temperature and (b4) 3 day sum of new snow height. (c) Evaluates the possibility of glide-snow avalanches due to melt based on its corresponding thresholds consisting of (c1) bulk snow density in combination with (c2) snow LWC, (c3) air temperature and (c4) soil LWC. (d) Evaluates the possibility of glide-snow avalanches due to rain (d1).

For the soil temperature and LWC measurements, we found that averaging data from at least five sensors with distances of several meters was essential to obtain robust time series that

reflected overall trends, without being influenced by local inhomogeneities. These inhomogeneities could arise from variations in soil properties or areas with preferential melt. While soil temperature

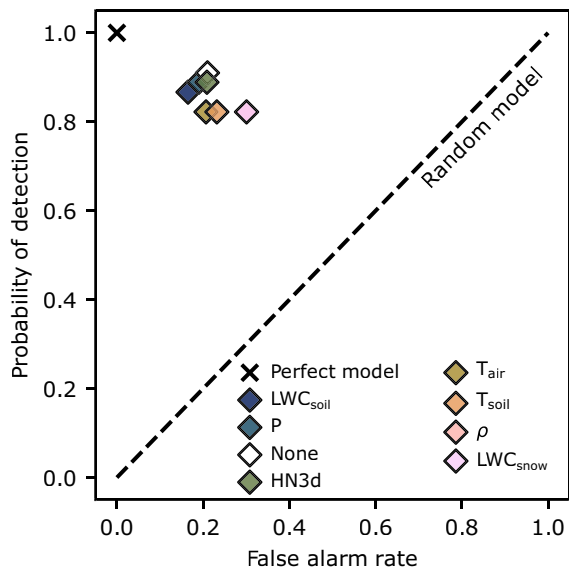


Figure 6. Performance of model with omission of input parameters. The omitted parameters (legend) were sorted in ascending Euclidean distance to the perfect model. The performances for the omission of ρ and LWC_{snow} were equal.

and LWC can be measured with a sensor at high time resolution and at reasonable cost, collecting data on the interfacial snow LWC is much more laborious. This currently limits the time resolution for snow LWC measurements to 5–9 days, which is a main limitation of the input data.

Measurements of soil LWC and rain did not contribute substantially to overall model performance (Fig. 6). However, they were essential input parameters to capture high glide-snow avalanche activity days such as the rain-on-snow event on 25 January 2024 (Fig. 5a). As the daily glide-snow avalanche activity did not influence the performance metric (POD, F) through the binary classification in avalanche and non-avalanche days, this likely underrepresented the importance of these input parameters.

The input data for the model were measured in proximity to the reference location, or interpolated to the reference location, and subsequently used to classify avalanche occurrence on all of Dorfberg. While this approach worked well overall, there are some limitations in the labeling of the glide-snow avalanche days. For example, some days (e.g. 19, 20 March 2024; Fig. 5a) were labeled as interface events because soil temperatures were high. This is likely not representative, as the Seewer Berg slope was only intermittently covered in snow, which caused an increase in soil temperature due to solar radiation. However, the glide-snow avalanches released on the fully snow-covered higher elevation slopes. This indicates that these glide-snow avalanches were likely surface events.

Overall, glide-snow avalanche occurrence on Dorfberg was classified based on simulations and measurements at one location. However, for regional forecasting, data from various aspects and elevations would be needed. Whenever possible, input parameters were based on SNOWPACK simulations, which are easily scalable for regional forecasting. Currently, however, the main challenge towards regional forecasting is obtaining high spatial and temporal information on the snow LWC. The (bi-)weekly manual snow profiles, which included interfacial snow LWC measurements at the reference location, provided valuable data to classify the avalanche activity on all of Dorfberg. In the future, the spatial and temporal resolution of snow LWC data could be improved through validated

simulations of water transport across the snow-soil systems. These simulations could be initiated with local soil temperature and LWC measurements.

4.3. Limitations in model generalization

The non-crossvalidated model performance suggests that the combination of soil, snow and meteorological measurements provides valuable information to predict glide-snow avalanche occurrence. However, this approach risks overfitting the data and currently limits the generalization of the model. Regarding the generalization, we expect that the best threshold vector depends on whether the input time series originate from measurements or simulations. Consequently, the best threshold vector cannot easily be generalized to other locations or datasets. In the future, more measurements from Dorfberg and other sites will allow for more data-driven methods, such as logistical regression or random forests, including training/testing splits and cross-validation. These methods could help to refine the thresholds into probabilities or provide the possibility of new model approaches. However, the results demonstrate that combining soil, snow and meteorological measurements with process-based understanding offers a promising foundation for future model development.

5. Conclusions and outlook

We developed an explanatory modeling approach combining soil, snow and meteorological measurements with process-based understanding towards improving glide-snow avalanche forecasting. The model provides a classification of glide-snow avalanche occurrence into days with and without avalanches using data from 3 seasons covering above-average, below-average, and average avalanche activity on Dorfberg (Davos, Switzerland). For classification, the model considers ten thresholds for eight variables closely linked to the three process drivers: geothermal heat, melt and rain. The best-performing threshold values were in line with field observations and previous studies. This indicates that the selected proxies may well capture the processes associated with the formation of interfacial water. These results show that measurements such as soil temperature, soil LWC and snow LWC contribute to improved glide-snow avalanche forecasting. For regional forecasting, additional measurements across elevations and aspects are needed, along with more high-resolution snow LWC data. As more data become available through continued measurements or improved snowpack simulations, data-driven methods (e.g. logistic regression, random forest) could refine the model and enhance forecasting accuracy. Overall, this study demonstrates that combining process understanding with soil and snow monitoring offers a solid foundation for advancing glide-snow avalanche prediction and provides the first process-based model for glide-snow avalanche activity which could be applied with climate change scenarios to assess their future behavior.

Data availability statement. All sensor measurements are available on Envidat (Fees and others, 2025b).

Acknowledgements. This research was supported by the Swiss National Science Foundation (grant no. 200021-212949). Color maps by Crameri and others (2020).

Author contributions. Conceptualization: all authors, Methodology: all authors, Formal analysis: A.F., Investigation: A.F., Data Curation: A.F.,

Writing—original draft: A.F., Writing—review & editing: all authors, Visualization: A.F., Supervision: A.H., J.S., Funding acquisition: J.S.

Funding statement. This research was supported by the Swiss National Science Foundation (grant no. 200021-212949).

Competing interests. The authors declare to have no competing interests.

References

- Bartelt P and Lehning M** (2002) A physical SNOWPACK model for the Swiss avalanche warning: Part I: numerical model. *Cold Regions Science and Technology* **35**(3), 123–145. doi: [10.1016/S0165-232X\(02\)00074-5](https://doi.org/10.1016/S0165-232X(02)00074-5)
- Ceaglio E, Mitterer C, Maggioni M, Ferraris S, Segor V and Freppaz M** (2017) The role of soil volumetric liquid water content during snow gliding processes. *Cold Regions Science and Technology* **136**, 17–29. doi: [10.1016/j.coldregions.2017.01.007](https://doi.org/10.1016/j.coldregions.2017.01.007)
- Clarke J and McClung D** (1999) Full-depth avalanche occurrences caused by snow gliding, Coquihalla, British Columbia, Canada. *Journal of Glaciology* **45**(151), 539–546. doi: [10.1017/S0022143000001404](https://doi.org/10.1017/S0022143000001404)
- Cramer F, Shephard GE and Heron PJ** (2020) The misuse of colour in science communication. *Nature Communications* **11**(1), 5444. doi: [10.1038/s41467-020-19160-7](https://doi.org/10.1038/s41467-020-19160-7)
- Denoth A** (1994) An electronic device for long-term snow wetness recording. *Annals of Glaciology* **19**, 104–106. doi: [10.3189/s0260305500011058](https://doi.org/10.3189/s0260305500011058)
- in der Gand H and Zupančič M** (1966) Snow gliding and avalanches. *Symposium at Davos 1965 – Scientific Aspects of Snow and Ice Avalanches*, IAHS Publication. International Association of Hydrological Sciences, Wallingford, Oxfordshire, UK. 230–242.
- Dreier L, Harvey S, van Herwijnen A and Mitterer C** (2016) Relating meteorological parameters to glide-snow avalanche activity. *Cold Regions Science and Technology* **128**, 57–68. doi: [10.1016/j.coldregions.2016.05.003](https://doi.org/10.1016/j.coldregions.2016.05.003)
- Fees A, Lombardo M, van Herwijnen A, Lehmann P and Schweizer J** (2025a) The source, quantity, and spatial distribution of interfacial water during glide-snow avalanche release: experimental evidence from field monitoring. *The Cryosphere* **19**(3), 1453–1468. doi: [10.5194/tc-19-1453-2025](https://doi.org/10.5194/tc-19-1453-2025)
- Fees A, Lombardo M, van Herwijnen A, Lehmann P and Schweizer J** (2025b) Spatio-temporal soil and local snow monitoring in a glide-snow avalanche prone slope above Davos Switzerland. *Envidat [data set]* doi: [10.16904/envidat.583](https://doi.org/10.16904/envidat.583)
- Fees A, van Herwijnen A, Altenbach M, Lombardo M and Schweizer J** (2025c) Glide-snow avalanche characteristics at different timescales extracted from time-lapse photography. *Annals of Glaciology* **65**, e3. doi: [10.1017/aog.2023.37](https://doi.org/10.1017/aog.2023.37)
- Fierz C and 8 others** (2009) The international classification for seasonal snow on the ground. *UNESCO, IHP-VII, Technical Documents in Hydrology, No 83; IACS Contribution No 1*, 80.
- Fromm R, Baumgärtner S, Leitinger G, Tasser E and Höller P** (2018) Determining the drivers for snow gliding. *Natural Hazards and Earth System Sciences* **18**(7), 1891–1903. doi: [10.5194/nhess-18-1891-2018](https://doi.org/10.5194/nhess-18-1891-2018)
- Höller P** (2001) Snow gliding and avalanches in a south-facing larch stand. In Dolman AJ, Hall AJ, Kavvas ML, Oki T and Pomeroy JW (eds.), *Soil-Vegetation-Atmosphere Transfer Schemes and Large-Scale Hydrological Models*, IAHS Publ. 270. International Association of Hydrological Sciences, Wallingford, Oxfordshire, U.K., pp. 355–358.
- Höller P** (2014) Snow gliding and glide avalanches: A review. *Natural Hazards* **71**(3), 1259–1288. doi: [10.1007/s11069-013-0963-9](https://doi.org/10.1007/s11069-013-0963-9)
- Humstad T, Dahle H, Orset KI, Venås M and Skrede I** (2018) The Stabrekka glide avalanche in Norway—evaluation after three years of monitoring. In Fischer JT, Adams M, Dobsberger P, Fromm R, Gobiet A, Granig M, Mitterer C, Nairz P, Tollinger C and Walcher M (eds.), *Proceedings ISSW 2018. International Snow Science Workshop, Innsbruck, Austria, 7–12 October 2018*, pp. 457–461.
- Jones AST** (2004) Review of glide processes and glide avalanche release. *Avalanche News, Canadian Avalanche Association* **69**, 53–60.
- Lombardo M, Fees A, Udke A, Meusburger K, van Herwijnen A, Schweizer J and Lehmann P** (2025) Capillary suction across the soil-snow interface as a mechanism for the formation of wet basal layers under gliding snowpacks. *Journal of Glaciology* **71**, e23. doi: [10.1017/jog.2025.2](https://doi.org/10.1017/jog.2025.2)
- Maggioni M, Godone D, Frigo B and Freppaz M** (2019) Snow gliding and glide-snow avalanches: Recent outcomes from two experimental test sites in Aosta Valley (northwestern Italian Alps). *Natural Hazards and Earth System Sciences* **19**(11), 2667–2676. doi: [10.5194/nhess-19-2667-2019](https://doi.org/10.5194/nhess-19-2667-2019)
- McClung D** (1987) Mechanics of snow slab failure from a geotechnical perspective. In Salm B and Gubler H (eds.), *Proceedings of the Symposium, Davos, International Association of Hydrological Sciences Publication*. International Association of Hydrological Sciences, Wallingford, Oxfordshire, UK. 475–508.
- Meter Group** (2025) *Instruction manual: TEROS11/12*, Meter Group. https://publications.metergroup.com/Manuals/20587_TEROS11-12_Manual_Web.pdf (accessed 1 June 2025).
- Mitterer C and Schweizer J** (2012) Glide snow avalanches revisited. *The Avalanche Journal* **102**, 68–71.
- Newesely C, Tasser E, Spadinger P and Cernusca A** (2000) Effects of land-use changes on snow gliding processes in alpine ecosystems. *Basic and Applied Ecology* **1**(1), 61–67. doi: [10.1078/1439-1791-00009](https://doi.org/10.1078/1439-1791-00009)
- Resch FJ, Bair E, Peitzsch E, Miller Z, Fees A, van Herwijnen A and Reiweger I** (2023) Comparison of the glide activity at two distinct regions using Swiss and U.S. datasets, *Proceedings ISSW 2023. International Snow Science Workshop, Bend, Oregon, U.S.A., 8–13 October 2023*, pp. 144–149.
- Sharaf D, Glude B and Janes M** (2008) Snettisham powerline avalanche—Juneau, Alaska. *The Avalanche Review* **27**(2), 1, 20.
- Simenhois R and Birkeland K** (2010) Meteorological and environmental observations from three glide avalanche cycles and the resulting hazard management technique. In *Proceedings ISSW 2010. International Snow Science Workshop*. Lake Tahoe CA, U.S.A., 17–22 October 2010, pp. 846–853.
- Sobol IM** (1967) The distribution of points in a cube and the accurate evaluation of integrals. *USSR Computational Mathematics and Mathematical Physics* **7**(4), 86–112.
- Stimberis J and Rubin CM** (2011) Glide avalanche response to an extreme rain-on-snow event. *Journal of Glaciology* **57**(203), 468–474. doi: [10.3189/002214311796905686](https://doi.org/10.3189/002214311796905686)
- Wilks DS** (2011) *Statistical Methods in the Atmospheric Sciences*. 4th ed. Amsterdam, Netherlands: Elsevier. 818.
- Zweifel B, Techel F, Marty C and Stucki T** (2025) *Schnee und Lawinen in den Schweizer Alpen. Hydrologisches Jahr 2023/24*. Birmensdorf, Switzerland: WSL Berichte, 160. doi: [10.55419/wsl:38525](https://doi.org/10.55419/wsl:38525)

Appendix A. Model performance for season 2021/22 and 2022/23

For season 2021/22, the model with the best threshold vector (Table 2) was able to predict the two clusters of glide-snow avalanche activity (11 to 16 Dec 2021 and 16 to 19 Mar 2022, Fig. A1). In season 2022/23, only one glide-snow avalanche released on Dorfberg, which was not predicted by the threshold model (17 Apr 2023, Fig. A2). However, this glide-snow avalanche released in a location which is known for its ground-water source and water at the soil surface. The model does not take into account groundwater as a source for interfacial water. This could explain why it was not able to predict the avalanche.

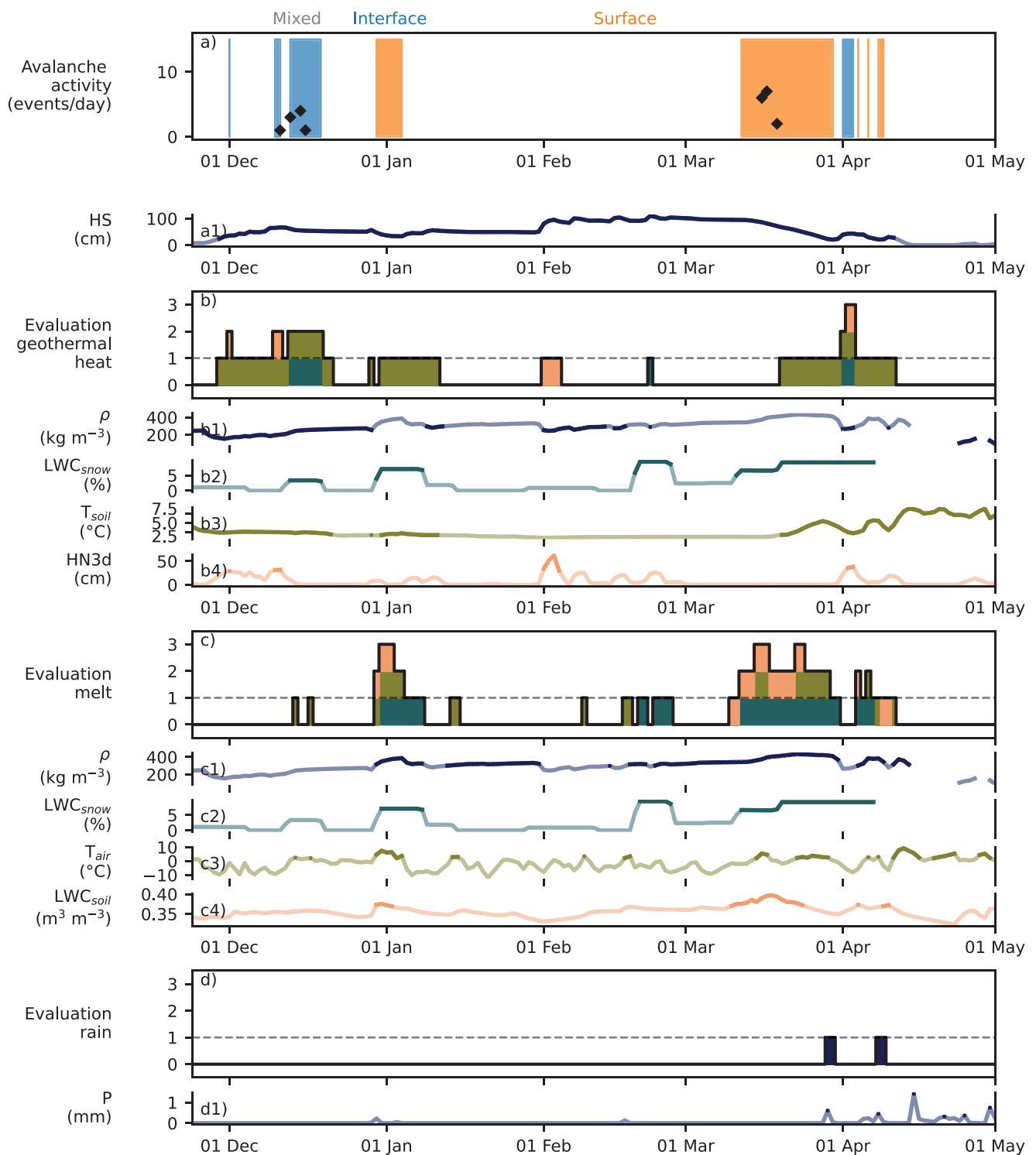


Figure A1. Model evaluation throughout season 2021/22. (a) Modeled glide-snow avalanche days (background color) in comparison to observed glide-snow avalanche activity on Dorfborg (black diamonds). This classification is based on three evaluations (b, c, d) which are based on thresholds on ten measured or simulated time-series (a1, b1-4, c1-4, d1). (a1) Snow height (HS) is a necessary requirement for glide-snow avalanches. In the time-series, a darker shade indicates that the condition (here: $HS > t_{HS}$) was met, while a lighter shade indicates that the condition was not met. (b) Evaluates the possibility of glide-snow avalanches based on geothermal heat. The background color visualizes the contributing thresholds consisting of (b1) bulk snow density in combination with (b2) snow LWC, (b3) soil temperature and (b4) 3 day sum of new snow height. (c) Evaluates the possibility of glide-snow avalanches due to melt based on its corresponding thresholds consisting of (c1) bulk snow density in combination with (c2) snow LWC, (c3) air temperature and (c4) soil LWC. (d) Evaluates the possibility of glide-snow avalanches due to rain (d1).

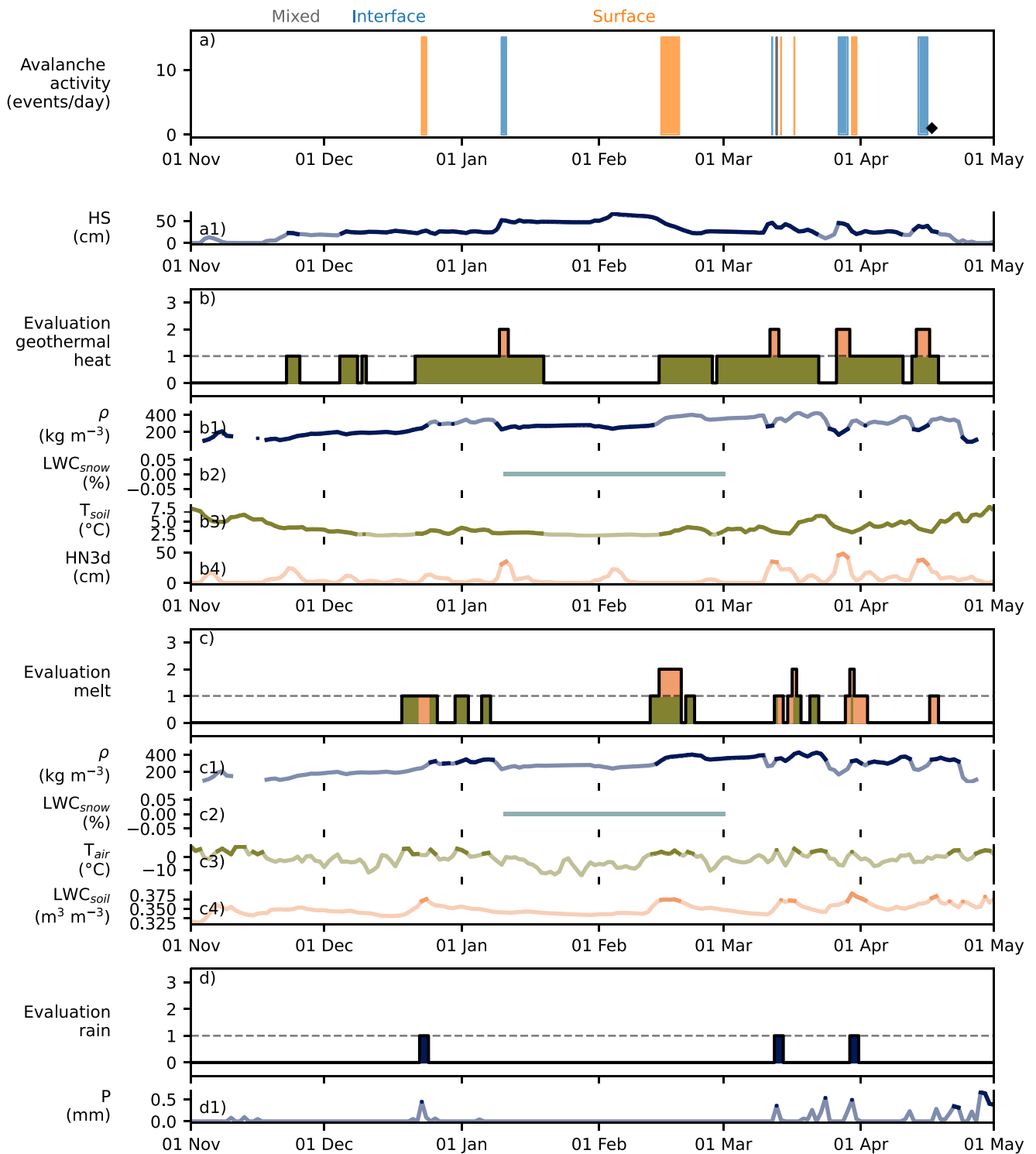


Figure A2. Model evaluation throughout season 2022/23. a) Modeled glide-snow avalanche days (background color) in comparison to observed glide-snow avalanche activity on Dorfborg (black diamonds). This classification is based on three evaluations (b, c, d) which are based on thresholds on ten measured or simulated time-series (a1, b1-4, c1-4, d1). (a1) Snow height (HS) is a necessary requirement for glide-snow avalanches. In the time-series, a darker shade indicates that the condition (here: $HS > t_{HS}$) was met, while a lighter shade indicates that the condition was not met. (b) Evaluates the possibility of glide-snow avalanches based on geothermal heat. The background color visualizes the contributing thresholds consisting of (b1) bulk snow density in combination with (b2) snow LWC, (b3) soil temperature and (b4) 3 day sum of new snow height. (c) Evaluates the possibility of glide-snow avalanches due to melt based on its corresponding thresholds consisting of (c1) bulk snow density in combination with (c2) snow LWC, (c3) air temperature and (c4) soil LWC. (d) Evaluates the possibility of glide-snow avalanches due to rain (d1).

A.1. Best thresholds

To determine the relative importance of the soil, snow and meteorological input time series, one time series was omitted at a time. The best-threshold vector was recalculated and is listed in [Table A1](#).

Table A1. The best threshold vector and its performance (POD, F) which was determined with one omitted time series at a time

Omitted variable	Best threshold vector										Performance	
	$t_{\text{LWC interface}}$	$t_{\text{LWC surface}}$	t_{soil}	t_{HN3d}	t_{air}	t_{LWCsoil}	t_{ρ}	t_{duration}	t_{p}	t_{HS}	POD	F
T_{soil}	3	6	NaN	29	2.0	0.369	287	4	0.9	20	0.82	0.23
LWC_{soil}	0	6	0.0	10	-1.0	NaN	200	0	0	20	0.87	0.16
P	3	6	0.1	29	2.0	0.369	287	NaN	NaN	20	0.89	0.19
HN3d	2	7	1.9	NaN	4.5	0.352	343	4	1.0	20	0.89	0.21
T_{air}	3	8	1.3	28	NaN	0.352	283	3	0.6	20	0.82	0.21
ρ	1	6	1.4	17	0.4	0.352	NaN	3	0.9	20	0.82	0.30
LWC_{snow}	NaN	NaN	1.4	17	0.4	0.352	222	3	0.9	20	0.82	0.30